Study of vibrational energy localization and redistribution in hydrogen peroxide H_2O_2 at low energy

Marc Joyeux[a)]
Laboratoire de Spectrométrie Physique (CNRS UMR 5588), Université Joseph Fourier—Grenoble 1, Boîte Postale 87, 38402 St Martin d'Hères, France

(Received 21 September 2004; accepted 1 December 2004; published online 4 February 2005)

Vibrational energy localization and/or redistribution in hydrogen peroxide H_2O_2 is studied at about 4000 cm^{-1} above the quantum mechanical ground state using the *ab initio* potential energy surface of Koput, Carter, and Handy [J. Phys. Chem. A **102**, 6325 (1998)]. In this work, the recently derived canonical perturbation procedure for floppy molecules serves two purposes. First, from the quantum mechanical point of view, it is shown that the energies of the lowest 130 states are reproduced with an average error smaller than 1.5 cm^{-1} by a two-dimensional Hamiltonian, which is a function of the torsion and OO-stretch coordinates and momenta, while the other four degrees of freedom contribute only through powers of good quantum numbers. Moreover, the canonical perturbation procedure is also used in classical mechanics calculations, in order to define meaningful local modes, for which the ingoing and outgoing energy flows are monitored. Almost all the individual trajectories launched on the *ab initio* surface display the same behavior, that is, the superposition of (a) rapid (few hundreds of femtoseconds) and quasiperiodic energy exchanges between the two OH stretches and between the torsion and OO-stretch, and (b) slower (few to several picoseconds) but erratic-looking energy flows between all degrees of freedom. When averaging over large numbers of trajectories with the same local mode energies at time $t=0$, one observes instead a smooth and irreversible energy flow between all degrees of freedom, which usually thermalize in the range of several tens of picoseconds, that is, on time scales larger than the 5 ps period associated with the quantum density of states. © *2005 American Institute of Physics*. [DOI: 10.1063/1.1850894]

I. INTRODUCTION

Intramolecular vibrational energy redistribution (IVR) studies are aimed at understanding the time evolution of the energy transiting in each vibrational degree of freedom of polyatomic molecules.[1–5] Thanks to refined laboratory techniques and increasing computational capabilities, experimental[6–12] as well as theoretical[13–21] description of IVR in molecular systems is becoming more precise and better documented. The present paper contributes to this effort by presenting a study of IVR in hydrogen peroxide H_2O_2 at about 4000 cm^{-1} above the quantum mechanical ground state. Hydrogen peroxide has recently received much attention from the theoretical point of view, with the construction of two *ab initio* potential energy surfaces (PESs),[22,23] which have both been shown to give accurate vibrational energy levels,[24–26] including correct estimates of the tunneling splittings through the torsional *trans* saddle. The two PESs are therefore more or less equivalent in the energy range investigated here, and the surface of Koput, Carter, and Handy[22,24] was chosen for its simplicity. Moreover, several theoretical studies have already dealt with IVR in H_2O_2 (see, for example, Refs. 13–16). They were essentially concerned with the dynamics at high energies, close to or above the dissociation threshold, and relied on simple, sometimes quasiseparable, model Hamiltonians. In contrast, the present study focuses on the dynamics at much lower energies on a realistic PES. Emphasis will be laid on two points.

First, most discussions dealing with IVR are based on plots showing the time evolution of the energies in so-called "local modes." Instead of energy, closely related quantities, such as classical action integrals or quantum numbers, are sometimes plotted. The important point, however, is that local modes are usually defined from the Hamiltonian of the system by fixing all coordinates, except for one, to some equilibrium value, and all momenta, except for the conjugate one, to zero. The definition of local modes is thus coordinate dependent, and different results must be expected when different sets of coordinates and conjugate momenta are used. A reasonable requirement for a coordinate system to be suitable for IVR studies is that the sum of local mode energies is not too different from the exact energy of the classical trajectory. It turns out that this requirement is very far from being fulfilled in H_2O_2 when using the "natural" set of valence coordinates, even in the rather low energy range investigated here. It will be shown that a solution to this problem consists in defining local modes after the recently derived canonical perturbation procedure for floppy molecules[27–29] has been applied to the exact Hamiltonian of the system.

The second point, which this study will insist on, concerns the quantum-classical correspondence during the IVR mechanism. Quantum mechanically, H_2O_2 looks like an integrable system up to at least 4000 cm^{-1} above the quantum mechanical ground state. Indeed, variational calculations on

a)Electronic mail: Marc.JOYEUX@ujf-grenoble.fr

the *ab initio* PES lead to regular wave functions and assignable quantum states.[24] Moreover, it will be shown in Sec. III, that the energies of the first 130 vibrational states are reproduced to within 3.7 cm^{-1} with a completely separable Hamiltonian. The classical system looks instead more complex. More precisely, the variations of local mode energies along classical trajectories launched on the *ab initio* PES (Ref. 22) clearly result from the superposition of two components, namely, (i) rapid (few hundreds of femtoseconds) and quasiperiodic energy oscillations between selected pairs of modes (the two OH stretches on one side, the O–O stretch and the torsion on the other side) and (ii) slower (several picoseconds) and erratic-looking flows between all the modes. While the rapid oscillations are due to a few low-order nonlinear resonances, the slower and erratic flows are a signature of the chaotic nature of the vibrational dynamics, because they result from a large number of weaker couplings between all the modes. It will be shown that classical and quantum mechanical results can be brought in better agreement by representing quantum states as an ensemble of classical trajectories with identical local mode energies at time $t=0$, but otherwise randomly chosen initial conditions. When averaging over large numbers of trajectories, local mode energies are seen to thermalize irreversibly in the time scale of several tens of picoseconds, which is substantially longer than the 5 ps period associated with the quantum density of states.

The remainder of this paper is organized as follows: the different canonical transformations, which are applied to the *ab initio* Hamiltonian, are briefly described in Sec. II. The quantum mechanical results obtained from perturbative calculations are next discussed in Sec. III, while Sec. IV is devoted to the classical analysis of IVR on the *ab initio* PES, with local modes however defined thanks to the perturbative Hamiltonian.

II. FROM THE *AB INITIO* PES TO THE PERTURBATIVE HAMILTONIANS

The canonical perturbation procedure for floppy molecules has already been described previously.[27–29] Therefore, it will only be summarized very briefly here (see the Appendix for few technical details). The basic idea is to apply a series of canonical transformations to the initial coordinates and momenta, in order to rewrite the Hamiltonian of the system in terms of as complete as possible a set of action integrals or, equivalently, good quantum numbers. It was shown, for example, that the vibrational degrees of freedom of HCN,[30] C_3,[31] and LiCN (Ref. 32) remain nearly separable up to their respective isomerization thresholds. As was also the case for the semirigid molecule CO_2,[33] the integrable approximations obtained from canonical perturbation theory (CPT) furthermore proved to be a keypoint for the investigation of monodromy in the floppy molecules HCN and LiCN.[32,34]

The starting point of CPT calculations is the *ab initio* Hamiltonian

$$H = T(p_{r_1}, p_{r_2}, p_R, p_{\theta_1}, p_{\theta_2}, p_\phi, r_1, r_2, R, \theta_1, \theta_2, \phi) + V(r_1, r_2, R, \theta_1, \theta_2, \phi), \tag{2.1}$$

where V is the potential energy surface of Koput, Carter, and Handy,[22] which is expressed as a function of the two OH bond lengths r_1 and r_2, the corresponding OOH bending angles θ_1 and θ_2, the OO bond length R, and the torsion angle ϕ. The expression of the kinetic energy T in terms of these coordinates and their conjugate momenta can be found, for example, in Ref. 35. Owing to the torsional dynamics of H_2O_2, ϕ is called the reactive coordinate, while the five other coordinates are described as spectator, or perpendicular, ones.

The reaction pathway, or minimum energy path (MEP), is defined, for each value of the torsion angle ϕ, as the set of the five perpendicular coordinates, which minimizes the potential energy surface V. The reaction-path Hamiltonian[36,37] is obtained by first rewriting the Hamiltonian of Eq. (2.1) in terms of the deviations of the perpendicular coordinates from their values on the MEP and then converting these deviations to normal mode coordinates thanks to Wilson's GF matrix procedure.[38] One thus obtains a reaction-path Hamiltonian of the form

$$H = T(P_1, P_2, P_3, p_\Phi, P_5, P_6, Q_1, Q_2, Q_3, \Phi, Q_5, Q_6) + V(Q_1, Q_2, Q_3, \Phi, Q_5, Q_6), \tag{2.2}$$

where $\Phi=\phi$ denotes the torsion angle, p_Φ its conjugate momentum [note that $p_\Phi \neq p_\phi$, see, for example, Eq. (2.3) of Ref. 29], and (P_k, Q_k) the dimensionless normal coordinates and momenta for symmetric OH stretch ($k=1$), symmetric OOH bend ($k=2$), OO stretch ($k=3$), antisymmetric OH stretch ($k=5$), and antisymmetric OOH bend ($k=6$). Up to this point, no approximation is made, except that the MEP transformation is applied to the classical Hamiltonian, not the quantum mechanical one, for the sake of simplicity.

After expanding the MEP Hamiltonian of Eq. (2.2) in Fourier series with respect to the torsion angle Φ and in Taylor series with respect to the five perpendicular coordinates, the canonical transformations described in Refs. 28 and 29 are applied in order to rewrite the Hamiltonian in terms of as complete as possible a set of good quantum numbers for the perpendicular degrees of freedom. Strictly speaking, the transformations of Refs. 28 and 29 are based on the quantum mechanical procedure pioneered by Van Vleck[39–41] and are thus used for the quantum mechanical calculations reported in Sec. III. The completely equivalent procedure based on Lie algebra and promoted by Dragt and Finn[42–45] is instead used for the classical mechanics calculations reported in Sec. IV. Note that the classical procedure is trivially obtained from the quantum mechanical one by replacing quantum commutators with Poisson brackets in all formulas. The transformed torsion angle and perpendicular dimensionless normal coordinates are denoted by τ and q_k ($k=1,2,3,5,6$), and their conjugate momenta by J and p_k. Moreover, the ladder operators (a_k, a_k^+) are defined according to

$$a_k = \frac{1}{\sqrt{2}}(q_k + ip_k),$$
$$a_k^+ = \frac{1}{\sqrt{2}}(q_k - ip_k), \tag{2.3}$$

the quantum numbers for the five perpendicular degrees of freedom according to $\nu_k = a_k^+ a_k$, and the classical action-angle coordinates (I_k, φ_k) according to

$$q_k = \sqrt{2I_k}\cos\varphi_k,$$
$$p_k = -\sqrt{2I_k}\sin\varphi_k. \tag{2.4}$$

The expression of the transformed (or *perturbative*) Hamiltonian depends on the coupling terms, which are taken into account. When neglecting all couplings, one obtains, for the quantum mechanical Hamiltonian,

$$H = \sum_{\mathbf{k},M,P,N} d_{\mathbf{k}MPN} \nu_1^{k_1} \nu_2^{k_2} \nu_3^{k_3} \nu_5^{k_5} \nu_6^{k_6} (\cos\tau)^M \sigma^P J^{2N}, \tag{2.5}$$

where the operator $\sigma = (\sin\tau)\partial/\partial\tau$ arises from the noncommutativity of $\cos(\tau)$ and J^2 (P is equal to 0 or 1), $\mathbf{k}$ is the vector $(k_1, k_2, k_3, k_5, k_6)$, and $d_{\mathbf{k}MPN}$ are real coefficients. The Hamiltonian of Eq. (2.5) is formally a one-dimensional Hamiltonian in the torsion degree of freedom parametrized by the values of the good quantum numbers ν_k for the five perpendicular degrees of freedom. If the 2:2 resonance between the two OH stretches (modes 1 and 5) is instead taken into account, then the perturbative Hamiltonian is of the form

$$H = \sum_{\mathbf{k},\mathbf{m},\mathbf{n},M,P,N} f_{\mathbf{kmn}MPN} \nu_2^{k_2} \nu_3^{k_3} \nu_6^{k_6} (a_1^+)^{m_1} \times a_1^{n_1} (a_5^+)^{m_5} a_5^{n_5} (\cos\tau)^M \sigma^P J^{2N}, \tag{2.6}$$

where $m_1 + m_5 = n_1 + n_5$. This Hamiltonian has only four good quantum numbers, namely, $\nu_1 + \nu_5$ (total OH stretch excitation), ν_2, ν_3, and ν_6. However, states which have less than two quanta in the OH stretches ($\nu_1 + \nu_5 < 2$) cannot be coupled by the Darling–Dennison resonance between modes 1 and 5, so that, for these states, ν_1 and ν_5 both remain good quantum numbers. Since the 130 states, which will be investigated in Sec. III, satisfy precisely $\nu_1 + \nu_5 < 2$, the Hamiltonian of Eq. (2.6) reduces, for these states, to the terms in Eq. (2.5) and is again formally one dimensional. At last, if the interactions between the OO stretch (mode 3) and the torsion (mode 4) are also taken into account, then the quantum mechanical perturbative Hamiltonian is of the form

$$H = \sum_{\mathbf{k},\mathbf{m},\mathbf{n},M,P,N} g_{\mathbf{kmn}MPN} \nu_2^{k_2} \nu_6^{k_6} (a_1^+)^{m_1} a_1^{n_1} \times (a_3^+)^{m_3} a_3^{n_3} (a_5^+)^{m_5} a_5^{n_5} (\cos\tau)^M \sigma^P J^{2N}, \tag{2.7}$$

where, again, $m_1 + m_5 = n_1 + n_5$. For states with less than two quanta of excitation in the OH stretches, the Hamiltonian of Eq. (2.7) is formally a two-dimensional Hamiltonian in the OO stretch and torsion degrees of freedom parametrized by the good quantum numbers ν_1, ν_2, ν_5, and ν_6 for the other degrees of freedom.

The classical perturbative Hamiltonians obtained from the procedure based on Lie algebra,[42–45] which is used in the classical mechanics study of Sec. IV, are of the same form as Eqs. (2.5)–(2.7), except that (a) there are no commutation problems, so that the terms in σ do not appear ($P = 0$), and (b) the expressions involve powers of the action integrals I_k rather than the good quantum numbers ν_k. These quantities are related through the Einstein–Brillouin–Keller[46–48] (EBK) semiclassical quantization rules,

$$I_k = \nu_k + \tfrac{1}{2}. \tag{2.8}$$

III. QUANTUM MECHANICAL ANALYSIS

This section is devoted to a discussion of the quantum mechanical results obtained from perturbative calculations.

The numerical values for the fundamental frequencies of the perpendicular degrees of freedom, which are obtained from Wilson's GF matrix procedure,[38] are $\omega_1 = 3810\ \text{cm}^{-1}$ (symmetric OH stretch), $\omega_2 = 1408\ \text{cm}^{-1}$ (symmetric OOH bend), $\omega_3 = 910\ \text{cm}^{-1}$ (OO stretch), $\omega_5 = 3807\ \text{cm}^{-1}$ (antisymmetric OH stretch), and $\omega_6 = 1363\ \text{cm}^{-1}$ (antisymmetric OOH bend). Since the two OH stretch frequencies are so close, the 2:2 resonance between these two degrees of freedom necessarily has to be taken into account in the course of perturbative calculations, in order for the asymptotic series not to diverge immediately, despite the fact that the two stretches have no atom in common and the direct coupling is consequently very small. When doing so, the perturbative Hamiltonian is of the form shown in Eq. (2.6). However, as already stressed in Sec. II, all states reported in Ref. 24 satisfy $\nu_1 + \nu_5 < 2$. Therefore, these states cannot be coupled by the 2:2 Darling–Dennison resonance and, in this energy range ($E \leqslant 4000\ \text{cm}^{-1}$), the perturbative Hamiltonian is formally one-dimensional in the torsion degree of freedom. The average absolute error between the energies of the first 130 states of H_2O_2 reported in Ref. 24 and those obtained from the perturbative Hamiltonian of Eq. (2.6) is $5.53\ \text{cm}^{-1}$ at second order of CPT, $3.71\ \text{cm}^{-1}$ at fourth order, and $4.52\ \text{cm}^{-1}$ at sixth order. It is therefore concluded that the various degrees of freedom of hydrogen peroxide remain almost decoupled in the whole energy range under investigation.

Nonetheless, it is possible from the plot of the errors to surmise the most important coupling, which takes place below $4000\ \text{cm}^{-1}$. Examination of the top plot of Fig. 1, which displays the errors at fourth order of CPT as a function of the energy of each state, indeed shows that the largest errors systematically occur in pairs of one positive and one negative values with approximately the same norm. Since, in addition, this always happens for states which differ by one quantum in the OO stretch and four quanta in the torsion, one might easily infer that these errors are due to the coupling between the OO stretch and the torsion degrees of freedom. Interestingly, Guo and co-workers[25,26] have shown that this resonance is also observed in the *ab initio* surface of Kuhn *et al.*[23] When taking all such couplings into account in CPT calculations, one obtains the two-dimensional perturbative Hamiltonian of Eq. (2.7). For this Hamiltonian, the average absolute error for the first 130 states of H_2O_2 is

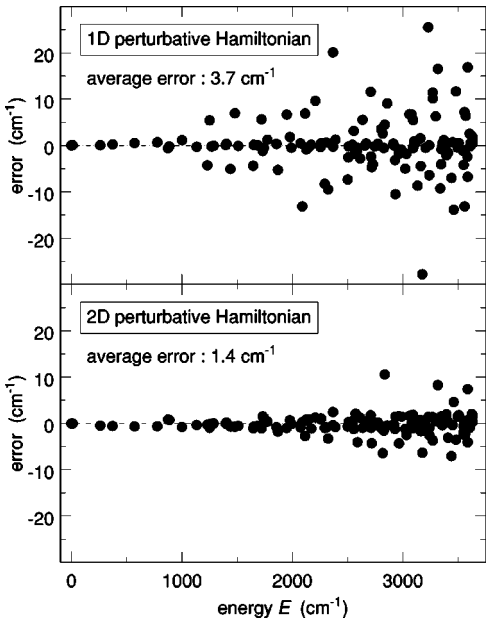

FIG. 1. Plot, as a function of energy of the errors between variational and perturbative eigenvalues for the first 130 states of H_2O_2 reported in Ref. 24. These states have up to 16 quanta of excitation in the torsion degree of freedom and $\approx$4000 cm^{-1} of vibrational excitation above the quantum mechanical ground state. The top plot shows the errors for the one-dimensional perturbative Hamiltonian of Eq. (2.6) at fourth order of the theory, while the bottom plot shows the errors for the two-dimensional Hamiltonian of Eq. (2.7), also at fourth order of CPT theory.

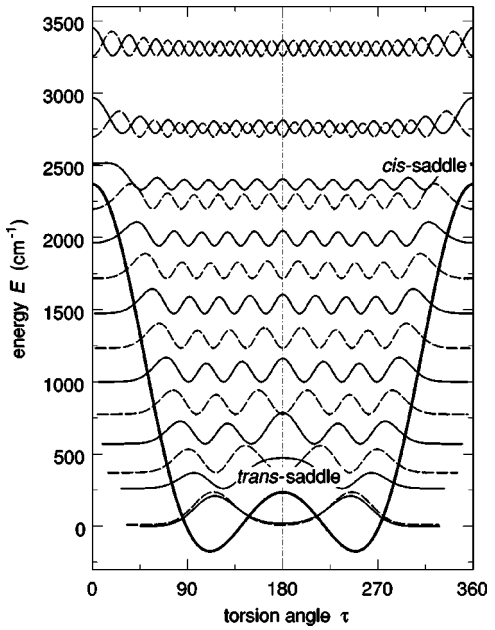

FIG. 2. Plot of the pseudopotential curve (thick line) and probability densities (thinner lines) for the pure torsion states ($\nu_1=\nu_2=\nu_3=\nu_5=\nu_6=0$) of H_2O_2 vs torsion angle τ. These results were obtained by applying fourth order CPT to the *ab initio* surface of Koput and co-workers (Refs. 22 and 24). The vertical scale is the same for all probability plots, while the baseline for each plot coincides with the energy of the state. The origin of the energy axis is taken at the quantum mechanical ground state.

6.69 cm^{-1} at second order of CPT, 1.41 cm^{-1} at fourth order, and 1.71 cm^{-1} at sixth order. The plot of the errors at fourth order of CPT as a function of the energies is shown in the bottom plot of Fig. 1. It was tried to improve further this excellent agreement by considering the couplings to the other degrees of freedom, but this proved to be unsuccessful. Therefore, the errors in the bottom plot of Fig. 1, the largest of which are observed for states with lots of quanta in the torsion degree of freedom, are very likely due to the approximations in getting the reaction-path Hamiltonian, that is, to the classical canonical transformation leading from Eq. (2.1) to Eq. (2.2) and the subsequent approximate symmetrization.

In order to help visualize more clearly what happens in hydrogen peroxide, one can plot the pseudopotential energy curves, obtained by setting $P=N=0$ in Eq. (2.5), for each set of quantum numbers $(\nu_1,\nu_2,\nu_3,\nu_5,\nu_6)$, as well as the corresponding one-dimensional wave functions. Such a plot is given in Fig. 2 for the pure torsion states $\nu_1=\nu_2=\nu_3=\nu_5=\nu_6=0$. In this figure, the thick line is the pseudopotential energy curve, while the thinner lines are the one-dimensional (1D) perturbative wave functions for the first 17 pure torsion states reported in Ref. 24. The pseudopotential energy curve displays two saddles, the *trans* saddle located only a few hundreds of cm^{-1} above the quantum mechanical ground state, and the higher *cis* saddle located about 2500 cm^{-1} above the quantum mechanical ground state. Consequently, the torsion states display a very peculiar energy pattern: the ground state, which is located below the *trans* saddle, appears as a doublet; there are then roughly ten nearly equally spaced vibrational-like states, which are located between the energies of the two saddles; finally, rotationlike doublets are observed above the energy of the *cis* saddle. Since the same pattern is repeated for each set $(\nu_1,\nu_2,\nu_3,\nu_5,\nu_6)$ of perpendicular quantum numbers, one can convince himself of the validity of the separable model for H_2O_2 by plotting, for each set $(\nu_1,\nu_2,\nu_3,\nu_5,\nu_6)$, the ground state splitting obtained from variational calculations[24] as a function of the height of the *trans* saddle obtained from CPT calculations. Figure 3 indeed shows that there is, as expected, an exponential relation between these two quantities.

Finally, Fig. 4 shows a set of five wave functions for the two-dimensional perturbative Hamiltonian of Eq. (2.7), which are coupled by the 1:4 resonance between the OO stretch and the torsion degrees of freedom. As usual, the resonance is responsible for the wavy structure of the wave functions, which is observed in these plots.

IV. CLASSICAL ANALYSIS

This section presents the classical analysis of IVR in H_2O_2 at about 4000 cm^{-1} above the quantum mechanical ground state, according to the *ab initio* PES of Koput, Carter, and Hardy,[22] with local modes however defined thanks to the perturbative Hamiltonian. Indeed, vibrational energy redistribution is usually investigated by monitoring the amount of energy that flows in and out so-called local modes, which are defined from the Hamiltonian of the system by fixing all coordinates, except for one, to some equilibrium value, and all momenta, except for the conjugate one, to zero. The definition of local modes is thus strongly coordinate dependent. A reasonable requirement for a set of local modes to be suitable for IVR studies is that the sum of local mode energies is not too different from the exact energy of the classical tra-

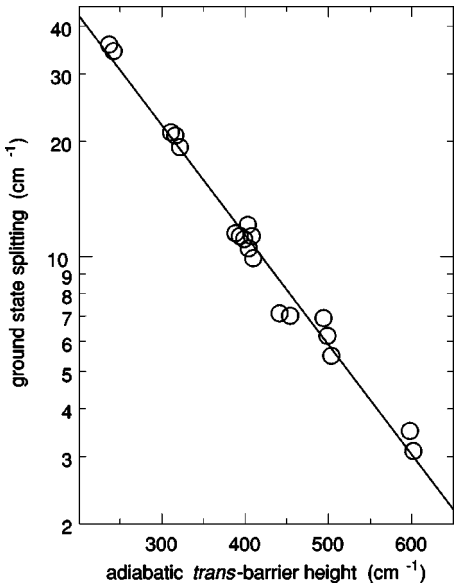

FIG. 3. Plot of the ground state energy splittings as a function of the height of the *trans* saddles. The ground state splittings, i.e., the energy gaps between the two lowest states with the same perpendicular quantum numbers $(\nu_1, \nu_2, \nu_3, \nu_5, \nu_6)$, were obtained from variational calculations on the *ab initio* PES and are reported in Ref. 24. In contrast, the height of the *trans* saddles was obtained from fourth order CPT calculations (see Fig. 2). The straight line is just a guide for the eyes, which is aimed at emphasizing the exponential relation between the two quantities.

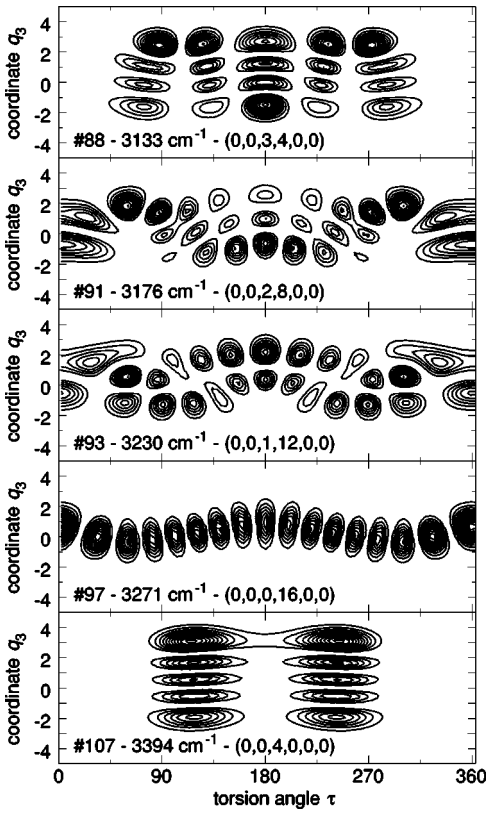

FIG. 4. Density probabilities for five states coupled by the 1:4 resonance between the OO stretch and torsion degrees of freedom, according to the two-dimensional Hamiltonian of Eq. (2.7) obtained at fourth order of CPT theory. τ is the torsion angle and q_3 the OO stretch dimensionless normal coordinate. Numbering, energy above the quantum mechanical ground state, and assignment are indicated for each state.

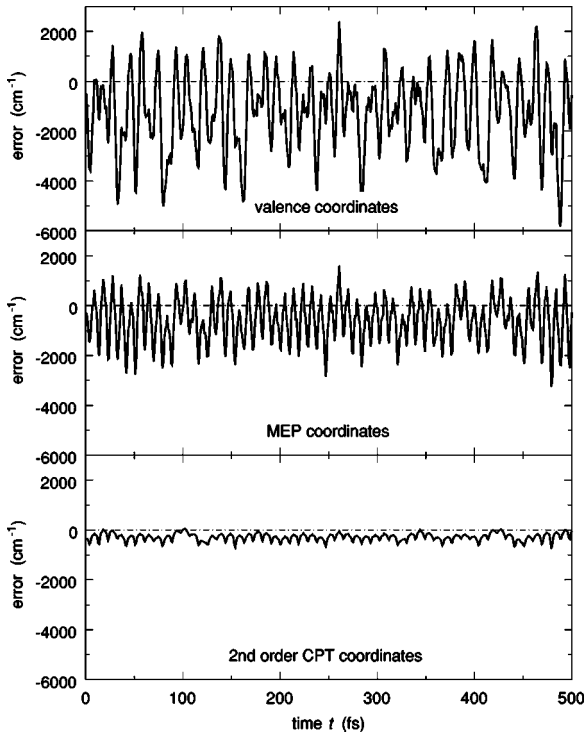

FIG. 5. Plot, as a function of time, from the difference between the energy of a given trajectory launched on the *ab initio* PES of Ref. 22 and the sum of local mode energies. From top to bottom, local modes are defined, respectively, from the valence coordinates of Eq. (2.1) (top plot), the reaction-path (or MEP) Hamiltonian coordinates of Eq. (2.2) (middle plot), and the coordinates of Eq. (2.6) obtained after two CPT transformations based on Lie algebra (bottom plot). The initial conditions of the trajectory were chosen, such that local mode energies at time $t=0$ correspond to the quantum state (0,2,1,0,0,0). This state is located at about 3600 cm^{-1} above the quantum mechanical ground state, that is, 9350 cm^{-1} above the bottom of the PES.

jectory. The top plot in Fig. 5 shows that this is far from being the case in H_2O_2 when using the valence coordinates of Ref. 22, that is, when defining local modes from the Hamiltonian of Eq. (2.1). This plot shows the variations, over a 500 fs time range, of the difference between the energy of a given trajectory launched on the *ab initio* PES (Ref. 22) and the sum of local mode energies defined from Eq. (2.1). This trajectory, for which local mode energies at time $t=0$ correspond to the quantum state (0,2,1,0,0,0), is located at about 3600 cm^{-1} above the quantum mechanical ground state, that is, at about 9350 cm^{-1} above the bottom of the PES (the ground state is calculated at 5950 cm^{-1} above the bottom of the PES). It is seen in the top plot of Fig. 1 that the fluctuations are as large as the energy of the trajectory itself, which indicates that the local modes used here are essentially meaningless. As shown in the middle plot of Fig. 5, the amplitude of the fluctuations is reduced by a factor of about 2 when using the coordinates of the reaction-path Hamiltonian, that is, when defining local modes from Eq. (2.2). The fluctuations are however still much too large for the purpose of trustful conclusions. In contrast, it is seen in the bottom plot of Fig. 5 that the amplitude of the fluctuations is very strongly reduced when using the perturbative coordinates obtained from CPT calculations, that is, when defining local modes from Eq. (2.6). Since this plot was obtained from

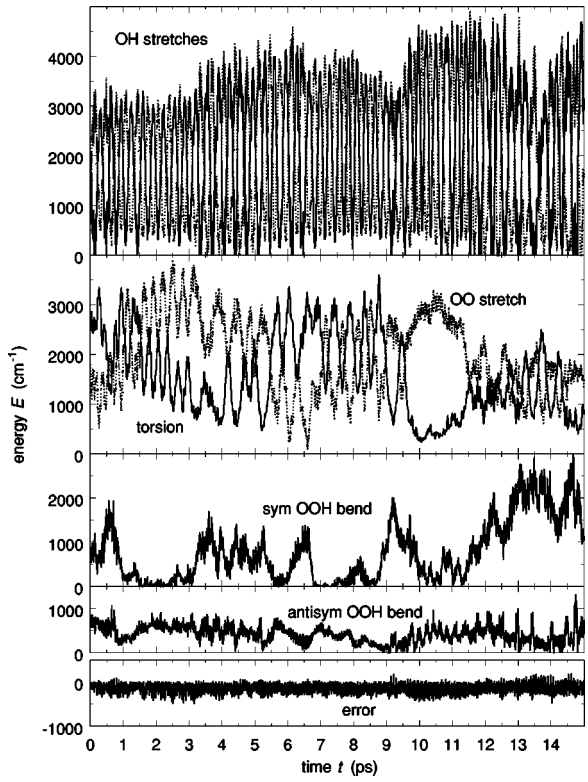

FIG. 6. Plot, as a function of time, of the local mode energies for a single trajectory launched on the *ab initio* PES (Ref. 22). Local modes are defined from the second order perturbative Hamiltonian of Eq. (2.6). The initial conditions of the trajectory were chosen, such that local mode energies at time $t=0$ correspond to the quantum state (0,0,1,12,0,0). This state is located at about 3200 cm^{-1} above the quantum mechanical ground state, that is, 8950 cm^{-1} above the bottom of the PES. From top to bottom, the plots show the local mode energies in the two OH stretches, the OO stretch and the torsion, the symmetric OOH bend, the antisymmetric OOH bend, and finally the difference between the exact energy of the trajectory and the sum of local mode energies.

second order CPT calculations (classical Lie method), it can furthermore be concluded that third and fourth order off-diagonal anharmonicities are responsible for the wild oscillations observed in the two upper plots.

In the remainder of this section, local modes are thus defined from the second order perturbative Hamiltonian of Eq. (2.6). The typical time evolution of local mode energies is shown in Fig. 6 for a single trajectory launched on the *ab initio* PES. Initial conditions for this trajectory were chosen such that local mode energies at time $t=0$ correspond to the quantum state (0,0,1,12,0,0), which is located at about 3200 cm^{-1} above the quantum mechanical ground state. Figure 6 very clearly illustrates that the time series consists of two components. The first component is a fast (few hundreds of femtoseconds) and quasiperiodic energy exchange between the two OH stretches, on one side, and between the OO stretch and the torsion, on the other side. Quite interestingly, these are precisely the two interactions, which must be taken into account in quantum mechanical calculations (see Sec. III). In addition, one also observes in Fig. 6 slower (few to several picoseconds) and erratic-looking energy flows between all local modes. These erratic flows are the signature of the chaotic nature of the classical dynamics of H_2O_2 even at these moderate energies. The exact extent of the chaotic portion of the phase space is hard to estimate for systems with six degrees of freedom. It was checked that islands of stability do survive at the investigated energies: for example, if one puts at time $t=0$ all the energy in one local mode, then it remains localized there. This implies that, at about 4000 cm^{-1} above the quantum mechanical ground state, each local mode is still surrounded by a stable island. Nonetheless, time evolutions similar to Fig. 6 were obtained for all trajectories mimicking a quantum state. As was already observed for HOCl (Refs. 49 and 50) and ozone,[51,52] this classically chaotic behavior is in clear contradiction with both variational quantum mechanical calculations, which lead to assignable quantum states,[24] and the perturbative calculations of Sec. III, which show that the energies of the first 130 vibrational states are reproduced to within 3.7 cm^{-1} with a completely separable Hamiltonian. As for HOCl,[49,50] this discrepancy might in part be due to the fact that quantum wave functions, for some not completely clear reason, could be more sensitive to the (eventually small) stable islands surrounding the local modes than to the rest of the chaotic sea.

However, another reason for this discrepancy is certainly that a quantum state should not be mimicked by a single classical trajectory, but instead by the average over many trajectories with initially the same local modes energies, as was done, for example, in Refs. 13 and 17. The results of such calculations are reported in Fig. 7, which shows the time evolution, averaged over 100 trajectories, of local mode energies. For each plot, the initial conditions of the 100 trajectories were chosen from a random procedure, which however ensures that local mode energies at time $t=0$ correspond to a given quantum state. From top to bottom, the considered quantum states are (1,0,0,0,0,0) ($E=3624$ cm^{-1}), (0,2,1,0,0,0) ($E=3609$ cm^{-1}), (0,0,4,0,0,0) ($E=3394$ cm^{-1}), and (0,0,1,12,0,0) ($E=3230$ cm^{-1}). It is seen that, despite the rather low total energy, the averaged system thermalizes smoothly and irreversibly, instead of wandering erratically as in Fig. 6. Moreover, it usually takes several tens of picoseconds for the system to reach thermal equilibrium. This is substantially longer than the 5 ps period associated with the quantum density of states at 4000 cm^{-1} above the quantum mechanical ground state, so that it is not completely surprising that the quantum states do not reflect all the complexity of the corresponding classical dynamics.

V. CONCLUSIONS

We have reported a combined quantum and classical study of IVR and localization in hydrogen peroxide at energies of about 4000 cm^{-1} above the ground state. The *ab initio* PES of Koput, Carter, and Handy[22,24] is used. In the first part of the paper, the canonical perturbation theory for floppy molecules[28,29] is employed, in order to derive 1D and 2D approximations of the 6D *ab initio* Hamiltonian. Comparison with the variational results of Koput, Carter, and Hardy[24] shows that the lowest 130 states of H_2O_2 are reproduced with respective average errors of 3.7 and 1.4 cm^{-1} by the 1D and 2D perturbative Hamiltonians. In the energy range considered, the vibrational modes of H_2O_2 are therefore essentially decoupled. The second part of the paper presents the results

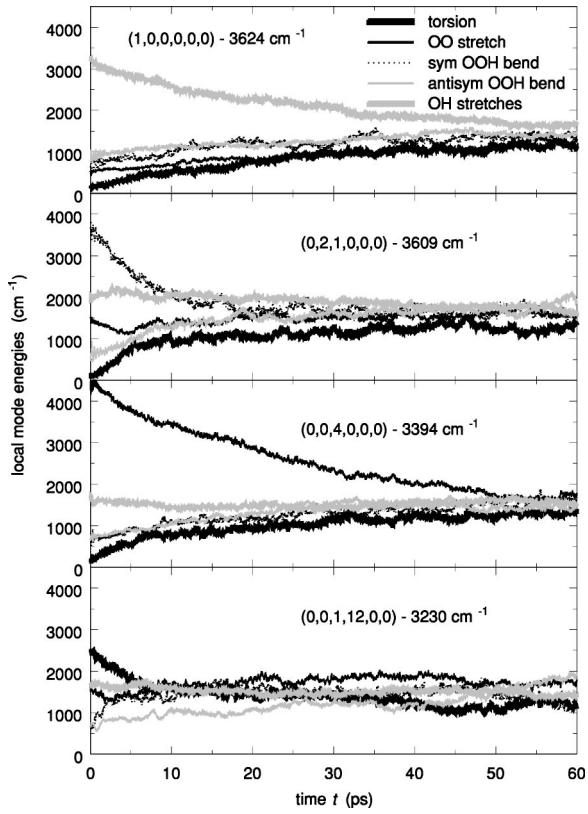

FIG. 7. Plots, as a function of time, of local mode energies averaged over 100 trajectories launched on the *ab initio* PES (Ref. 22). For each plot, the initial conditions of the 100 trajectories were chosen from a random procedure, which however ensures that local mode energies at time $t=0$ correspond to a given quantum state. From top to bottom, the considered quantum states are (1,0,0,0,0,0), (0,2,1,0,0,0), (0,0,4,0,0,0), and (0,0,1,12,0,0), respectively. Local modes are defined from the second order perturbative Hamiltonian of Eq. (2.6). Note that averaging over 100 trajectories cancels the greatest part of the 100% energy fluctuations between the two OH stretches (see the top plot of Fig. 6); nevertheless, for the sake of clarity, each plot does not show the energy in each OH stretch, but rather the mean energy in the two OH stretches.

of a complementary study of the classical IVR in the same energy range. A classical version of canonical perturbation theory is used to define meaningful local modes. Classically chaotic dynamical behavior is found, in contradiction to the assignable quantum eigenstates. Averaging the classical results over 100 trajectories for each quantum state reduces greatly the fluctuations and reveals decay times of the order of several tens of picoseconds, which might explain part of the distinction between quantum and classical results.

It is now planned to investigate whether CPT can also be used to study more complex floppy systems, such as for example molecules where, due to symmetry, several equivalent minimum energy paths exist (e.g., H_3^+), or molecules with several floppy modes, for which minimum energy *surfaces* must be considered (e.g., C_2H_2).

APPENDIX: DETAILS OF CPT CALCULATIONS

The principal difference between the torsion angle τ of the bent molecule H_2O_2 and the bending angle γ of linear molecules such as HCN or LiCN is that γ is doubly degenerate, while τ is not. Therefore, in the case of H_2O_2, the operator J is taken to be just $-i\hbar\partial/\partial\tau$, so that the commutation relations in Eq. (4.5) of Ref. 28 must be slightly modified, according to

$$J^2(\cos\tau)^M = (\cos\tau)^M J^2 + 2M(\cos\tau)^{M-1}\sigma + M^2(\cos\tau)^M - M(M-1)(\cos\tau)^{M-2},$$

$$J^2(\cos\tau)^M\sigma = (\cos\tau)^M\sigma J^2 + 2(M+1)(\cos\tau)^{M+1}J^2 - 2M(\cos\tau)^{M-1}J^2 + (M+1)^2(\cos\tau)^M\sigma - M(M-1)(\cos\tau)^{M-2}\sigma, \tag{A1}$$

$$\sigma(\cos\tau)^M = (\cos\tau)^M\sigma + M(\cos\tau)^{M+1} - M(\cos\tau)^{M-1},$$

$$\sigma(\cos\tau)^M\sigma = (\cos\tau)^{M+2}J^2 - (\cos\tau)^M J^2 + (M+1)\times(\cos\tau)^{M+1}\sigma - M(\cos\tau)^{M-1}\sigma,$$

while the Hermitian conjugate of σ writes

$$\sigma^+ = -\sigma - \cos\tau. \tag{A2}$$

Note that for a nondegenerate torsion angle τ one can use the operators $\exp(\mp iM\tau)$ instead of the operators $(\cos\tau)^M$, but the commutation relations are then completely different. At last, it is emphasized that a computer code for the classical canonical perturbation procedure based on Lie algebra[42–45] is very simply obtained from the quantum mechanical procedure by canceling all reordering subroutines and implementing the relations

$$i\{(a^+)^m a^n, (a^+)^M a^N\} = (mN - nM)(a^+)^{m+M-1}a^{n+N-1},$$
$$i\{e^{ik\tau}J^n, e^{iK\tau}J^N\} = (kN - nK)e^{i(k+K)\tau}J^{n+N-1}. \tag{A3}$$

[1] A. Zewail, in *Femtochemistry*, edited by F. C. de Schryver and G. Schweitzer (Wiley, New York, 2001).
[2] T. Uzer, Phys. Rep. **199**, 73 (1991).
[3] K. Lehman, G. Scoles, and B. H. Pate, Annu. Rev. Physiol. **45**, 241 (1994).
[4] D. J. Nesbitt and R. W. Field, J. Phys. Chem. **100**, 12735 (1996).
[5] M. Gruebele and R. Bigwood, Int. Rev. Phys. Chem. **17**, 91 (1998).
[6] D. Romanini and A. Campargue, Chem. Phys. Lett. **254**, 52 (1996).
[7] O. Boyarkin, M. Kowalszyk, and T. Rizzo, J. Chem. Phys. **118**, 93 (2003).
[8] M. Coffey, H. Berghout, E. Wood, and F. Crim, J. Chem. Phys. **110**, 10850 (1999).
[9] A. Callegari, J. Rebstein, R. Jost, and T. Rizzo, J. Chem. Phys. **111**, 7359 (1999).
[10] O. Boyarkin, T. Rizzo, and D. Perry, J. Chem. Phys. **110**, 11346 (1999).
[11] B. Kuhn and T. Rizzo, J. Chem. Phys. **112**, 7461 (2000).
[12] A. Callegari, U. Merker, P. Engels, H. Srivastava, K. Lehman, and G. Scoles, J. Chem. Phys. **113**, 10583 (2000).
[13] T. Uzer, J. T. Hynes, and W. P. Reinhardt, J. Chem. Phys. **85**, 5791 (1986).
[14] B. G. Sumpter and D. L. Thompson, J. Chem. Phys. **86**, 2805 (1987).
[15] B. G. Sumpter and D. L. Thompson, Chem. Phys. Lett. **153**, 243 (1988).
[16] C. Getino, B. G. Sumpter, and J. Santamaria, Chem. Phys. **145**, 1 (1990).
[17] T. A. Holme and R. D. Levine, Chem. Phys. **131**, 169 (1989).
[18] V. Wong and M. Gruebele, J. Phys. Chem. A **103**, 10083 (1999).
[19] T. J. Minehardt, J. D. Adcock, and R. E. Wyatt, J. Chem. Phys. **110**, 3326 (1999).
[20] F. Richter, P. Rosmus, F. Gatti, and H.-D. Meyer, J. Chem. Phys. **120**, 6072 (2004).
[21] C. Iung, F. Gatti, and H.-D. Meyer, J. Chem. Phys. **120**, 6992 (2004).
[22] J. Koput, S. C. Carter, and N. C. Handy, J. Phys. Chem. A **102**, 6325 (1998).
[23] B. Kuhn, T. Rizzo, D. Luckaus, M. Quack, and M. A. Suhm, J. Chem. Phys. **111**, 2565 (1999).

[24]J. Koput, S. C. Carter, and N. C. Handy, J. Chem. Phys. **115**, 8345 (2001).
[25]R. Chen, G. Ma, and H. Guo, J. Chem. Phys. **114**, 4763 (2001).
[26]S. Y. Lin and H. Guo, J. Chem. Phys. **119**, 5867 (2003).
[27]D. Sugny and M. Joyeux, J. Chem. Phys. **112**, 31 (2000).
[28]M. Joyeux and D. Sugny, Can. J. Phys. **80**, 1459 (2002).
[29]M. Joyeux, S. Yu. Grebenshchikov, J. Bredenbeck, R. Schinke, and S. C. Farantos, Adv. Chem. Phys. **130**, 267 (2005).
[30]D. Sugny, M. Joyeux, and E. L. Sibert, J. Chem. Phys. **113**, 7165 (2000).
[31]J. Robert and M. Joyeux, J. Chem. Phys. **119**, 8761 (2003).
[32]M. Joyeux, D. A. Sadovskii, and J. Tennyson, Chem. Phys. Lett. **382**, 439 (2003).
[33]R. H. Cushman, H. R. Dulin, A. Giacobbe, D. D. Holm, M. Joyeux, P. Lynch, D. A. Sadovskii, and B. I. Zhilinskii, Phys. Rev. Lett. **93**, 024302 (2004).
[34]K. Efstathiou, M. Joyeux, and D. A. Sadovskii, Phys. Rev. A **69**, 032504 (2004).
[35]M. J. Bramley, W. H. Green, and N. C. Handy, Mol. Phys. **73**, 1183 (1991).
[36]W. H. Miller, N. C. Handy, and J. E. Adams, J. Chem. Phys. **72**, 99 (1980).
[37]S. Carter and N. C. Handy, J. Chem. Phys. **113**, 987 (2000).
[38]E. B. Wilson, J. C. Decius, and P. C. Cross, *Molecular Vibrations* (Dover, New York, 1955).
[39]J. H. Van Vleck, Phys. Rev. **33**, 467 (1929).
[40]E. C. Kemble, *The Fundamental Principles of Quantum Mechanics* (McGraw-Hill, New York, 1937), Sec. 48c.
[41]E. L. Sibert, J. Chem. Phys. **88**, 4378 (1988).
[42]A. J. Dragt and J. M. Finn, J. Math. Phys. **17**, 2215 (1976).
[43]A. J. Dragt and J. M. Finn, J. Math. Phys. **20**, 2649 (1979).
[44]J. R. Cary, Phys. Rep. **79**, 129 (1981).
[45]A. J. Dragt and E. Forest, J. Math. Phys. **24**, 2734 (1983).
[46]A. Einstein, Verh. Dtsch. Phys. Ges. **19**, 82 (1917).
[47]L. Brillouin, J. Phys. Radium **7**, 353 (1926).
[48]J. Keller, Ann. Phys. **4**, 180 (1958).
[49]M. Joyeux, D. Sugny, M. Lombardi, R. Jost, R. Schinke, S. Skokov, and J. Bowman, J. Chem. Phys. **113**, 9610 (2000).
[50]R. Jost, M. Joyeux, S. Skokov, and J. Bowman, J. Chem. Phys. **111**, 6807 (1999).
[51]M. Joyeux, R. Schinke, and S. Yu. Grebenshchikov, J. Chem. Phys. **120**, 7426 (2004).
[52]S. Yu. Grebenshchikov, R. Schinke, P. Fleurat-Lessard, and M. Joyeux, J. Chem. Phys. **119**, 6512 (2003).